10th World Congress on Structural and Multidisciplinary Optimization
May 19 -24, 2013, Orlando, Florida, USA

A Numerical Form Finding Method for Minimal Surface of Membrane Structure

Koichi Yamane[1], Masatoshi Shimoda[2]

[1] Toyota Technological Institute, Tenpaku-ku, Nagoya, Japan, xsdfghjkk@gmail.com
[2] Toyota Technological Institute, Tenpaku-ku, Nagoya, Japan, shimoda@toyota-ti.ac.jp

1. Abstract
This paper proposes a convenient numerical form-finding method for designing the minimal surface, or the equally tensioned surface of membrane structures with specified arbitrary boundaries. The area minimization problems are formulated as a distributed-parameter shape optimization problem. The internal volume or the perimeter is added as the constraints according to the structure type such as a pneumatic or a suspension membrane. It is assumed that the membrane is varied in the normal and/or the tangential direction to the surface. The shape sensitivity function for the problems is derived using the material derivative method. The minimal surface is determined without the shape parameterization by the free-form optimization method, a gradient method in a Hilbert space, where the shape is varied by the traction force in proportion to the sensitivity function under the Robin condition. The calculated results will show the effectiveness and practical utility of the proposed method for the optimal form-finding of membrane structures.
2. Keywords: Membrane structure, Form finding, Shape optimization, Minimal surface, Free form

3. Introduction
Sheet-like solid as cloth and resin film is called membrane, which is very thin and flexible. Mechanical characteristics of membrane structure are that its bending is negligible, while it keeps its shape and carries external force with the stress consisting of the in-plane tensile stress and the shear stress. Not only isotropic materials but anisotropic ones are used for membrane. Membrane structure has a lot of advantages: they contribute to safety and economy, they are light weight and not bulky, and they have good aesthetic aspects due to its curved surface and the translucency. Making good use of these characteristics or advantages, various membrane structures have been developed and widely used for industrial products. In the field of architecture, membranes tend to be used as roofs because of constructing long span structures, short construction period, and excellent earthquake resistance. They also can be functional structures because automotive air-bags absorb the impact energy, while the sails of yachts and the wings of paragliders generate the lifting power. Further, they're used as airship, balloon, playground equipment, and daily commodity (e.g. umbrella and chair).
As mentioned above, membranes need to be maintained their shapes only with the in-plane tension due to negligible bending stiffness, which makes themselves difficult to maintain the shapes as required. Therefore the form-finding is highly important in the design process. In order to keep the shape and to secure the sufficient stiffness and strength against self-weight and external force, initial tensions must to be appropriately applied to membranes. Membrane structures are classified into the pneumatic (air-support) membrane structure which tensions are generated by the differential pressure and the non-pneumatic membrane structure which tensions are applied by the mechanical force [1]. The non-pneumatic structures are also classified into the frame membrane structure and the suspension membrane structure. The non-pneumatic structures must have non-positive Gaussian curvature over the whole surface to maintain the shape. Fig. 1 shows the classification of membrane structures. Regardless of the structure type, we can't expect its bearing capacity that much due to its thinness even if the material of membrane itself is strong. Therefore designers are required to determine the shape so that the membrane has a uniform stress field throughout the surface.

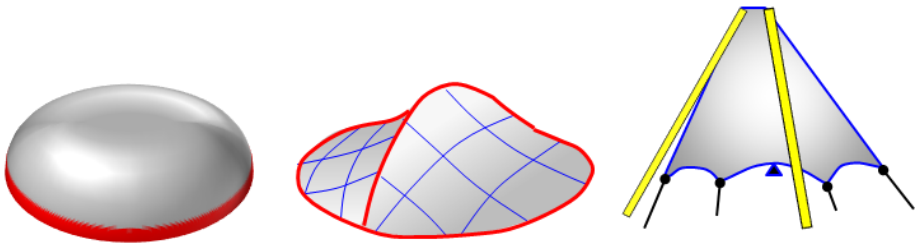

(a) Pneumatic membrane structure (b) Frame membrane structure (c) Suspension membrane structure
Figure 1: Classification of membrane structures

It's well known that a shape that has a uniform stress field conforms to the minimal surface which has zero mean curvature throughout the surface if the deformation due to the self-weight is negligible. In the case a constraint condition is given, it has a certain amount of the curvature. Such surface with a constant curvature is also regarded as the minimal surface under the constraint condition. Even though these surfaces are just ideal ones and different from the optimal shape subjected to an external force, they are considered as the base of an optimal shape. Therefore finding this basic shape is imperative, and many approaches using experiments and calculation have been done. A physical experiment as soap-film has been used for centuries as it can easily find minimal surfaces with frames [1]. It was also mathematically studied as a variational problem and many minimal surface functions were found [2]. However it's difficult to find minimal surfaces within arbitrary boundaries taking account of structural characteristics or aesthetic satisfaction. Thus the applicable range of the both approaches can never be extended. In order to get over the disadvantage, versatile numerical solutions making use of computer have been studied. Monterde [3] determined approximate minimal surfaces using Bezier surfaces, and Arnal et al. [4] also used them and obtained surfaces with a constant mean curvature. These are efficient methods since design variables were decreased by shape parameterization, while the obtained shape and its characteristics are restricted by the parameter. Bletzinger et al. [5] represented a method that simulates classical physical experiments as the soap-film and the hanging-model by the finite element analysis taking geometric non-linearity into consideration. It takes a lot of computation cost, yet it doesn't need shape parameterization and is applicable in the both cases that an anisotropic material is used and that an initial tension is applied. They also showed a method combined with mesh regularization. [6]

In the wake of these studies, in this paper we proposed a new numerical solution for finding a minimal surface, i.e. an equally tensioned surface, with an arbitrarily specified boundary. The authors have been developing numerical solutions for three-dimension continua [7], shell structures [8],[9] and frame structures [10] as a distributed-parameter free-form optimization method without shape parameterization. This study shows a numerical solution for form-finding of membrane structure by applying our shape optimization method for shell structures. This method finds a minimal surface by formulating the form-finding problem as the distributed-parameter shape optimization problem based on the variational method, and applying the sensitivity function derived by the material derivative method to the shape optimization method for shell structures. Advantages of this method are the efficiency against large-scale problems and that a smooth shape can be obtained. In the shape design of a membrane structure, the shape could vary in the in-plane direction and/or out-of-plane direction. We consider the both directions as design variables. Form-findings with constraint conditions (e.g. perimeter and internal volume) can be performed for a pneumatic membrane structure, a frame membrane structure and a suspension membrane structure.

In the following chapters, first we will show the formulations of minimal surface problems as the distributed-parameter optimization problem and derive the each sensitivity function which is called shape gradient function. Then the free-form optimization method for membrane structures will be proposed. Finally we will show the examples of each type of membrane structure.

4. Definition of shape variation for free-form design

As shown in Fig. 2, consider that a membrane having an initial domain A with the boundary ∂A is varied into the one having domain A_s with the boundary ∂A_s by the shape variation (the design velocity field) $\boldsymbol{V}$ distributed throughout the surface. It is assumed that the boundary ∂A is included in the domain A ($\partial A \subset A$) and that the thickness h is constant during the deformation. The shape variation $\boldsymbol{V}$ consists of the out-of-plane variation $\boldsymbol{V}_n$ which deforms in the normal direction to the surface and the in-plane direction $\boldsymbol{V}_t$ which deforms in the tangential direction to the surface. The membrane shape is varied by $\boldsymbol{V}_n(A)$ distributed on A and $\boldsymbol{V}_t(\partial A)$ distributed on ∂A since $\boldsymbol{V}_t(A)$ doesn't affect to the shape variation except on ∂A. The shape variation is expressed by the piecewise smooth mapping $T_S : \boldsymbol{X} \in A \mapsto \boldsymbol{X}_s(\boldsymbol{X}) \in A_s$, $0 \le s \le \varepsilon$ [9],[11], where ε and $(\cdot)_s$ indicate small integer and iteration history of the shape variation worth the time. With the relations $\boldsymbol{X}_s = T_s(\boldsymbol{X})$, $A_s = T_s(A)$, the small shape variation around the s-th variation is expressed as

$$T_{s+\Delta s}(\boldsymbol{X}) = T_s(\boldsymbol{X}) + \Delta s \boldsymbol{V} + O(|\Delta s|^2) \ , \tag{1}$$

where the design velocity field $\boldsymbol{V}(\boldsymbol{X}_s) = \partial T_s(\boldsymbol{X}) / \partial s$ is given as the Euler derivative of the mapping $T_s(\boldsymbol{X})$,and $O(|\Delta s|^2)$ is assumed to be neglected due to high-order term. The optimal design velocity field $\boldsymbol{V}(\boldsymbol{X}_s)$ is determined by the free-form optimization method proposed in this paper, which will be explained later.

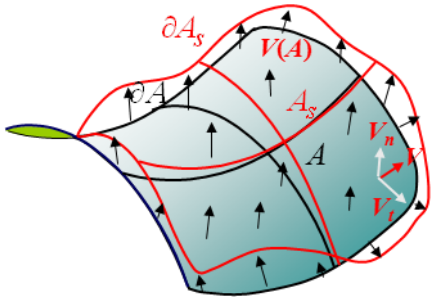

Figure 2: Shape variation of membrane by $\boldsymbol{V}$

5. Form-finding problems of membrane structures and derivation of shape gradient function

In order to find the minimal surface, the area of a membrane is set up as an objective functional. In addition to the boundary shape, internal volume or perimeter is set as another constraint condition according to the structure type. In this chapter, for the each structure type, we will formulate the distributed-parameter shape optimization problem so as to determine the design velocity field which leads to the minimal surface, and then the shape gradient function will be derived.

5.1. Frame membrane structure problem

Consider a shape optimization problem for minimizing the area of a frame membrane structure shown in Fig. 1(b). When an initial membrane shape A_0 and a specified boundary shape made of frame which may be open boundary are given, this problem is expressed as

$$\text{Given} \quad A_0\,, \tag{2}$$

$$\text{find} \quad \boldsymbol{V} \ (\text{or}\ A_s)\,, \tag{3}$$

$$\text{that minimizes} \quad A\,(=\int_A dA)\,. \tag{4}$$

The Lagrange functional L for this problem is expressed as

$$L(A) = \int_A dA\,. \tag{5}$$

The material derivative $\dot{L}$ of the Lagrange functional L with respect to shape variation is expressed as

$$\dot{L} = <\boldsymbol{G}_A n, \boldsymbol{V}>_A + <\boldsymbol{G}_{\partial A} t, \boldsymbol{V}>_{\partial A}, \quad \boldsymbol{V} \in C_\Theta, \tag{6}$$

where the notations of $<\boldsymbol{G}_A n, \boldsymbol{V}>_A$ and $<\boldsymbol{G}_{\partial A} t, \boldsymbol{V}>_{\partial A}$ are defined as

$$<\boldsymbol{G}_A n, \boldsymbol{V}>_A \equiv \int_A G_A \boldsymbol{n}\cdot\boldsymbol{V} dA = \int_A G_A \boldsymbol{V}_n dA\,, \tag{7}$$

$$<\boldsymbol{G}_{\partial A} t, \boldsymbol{V}>_{\partial A} \equiv \int_{\partial A} G_{\partial A} \boldsymbol{t}\cdot\boldsymbol{V} d\Gamma = \int_{\partial A} G_{\partial A} \boldsymbol{V}_t d\Gamma\,, \tag{8}$$

$$G_A = H_A, \quad G_{\partial A} = H_{\partial A}. \tag{9)(10}$$

C_Θ indicates the admissible function space which satisfies the specified geometric boundary condition. The coefficient functions G_A and $G_{\partial A}$ of velocity field components $\boldsymbol{V}_n$ and $\boldsymbol{V}_t$ are called shape gradient function and are distributed on the surface and on the boundary, respectively. Eq. (6), (9) and (10) imply that when the Lagrange functional L has the minimum (i.e. $\dot{L} = 0$), both the mean curvatures on the surface and the curvature on the boundary vanish (i.e. $H_A = H_{\partial A} = 0$). If the arbitrary boundary is closed one, second term of the right-hand side in Eq. (6) is omitted.

5.2. Pneumatic membrane structure problem

Consider a problem for minimizing the area of a pneumatic membrane structure subjected to differential pressure, which is shown in Fig. 1(a). Setting up respectively a specified boundary as the geometric constraint condition and an internal volume Ω (i.e. a space bounded by the membrane) as the equality constraint condition (the constraint value is represented as $\hat{\Omega}$), this problem is expressed as

$$\text{Given} \quad A_0, \tag{11}$$
$$\text{find} \quad \boldsymbol{V} \ (\text{or } A_s), \tag{12}$$
$$\text{that minimizes} \quad A \left(=\int_A dA\right), \tag{13}$$
$$\text{subject to} \quad \Omega \left(=\int_\Omega d\Omega\right) = \hat{\Omega}. \tag{14}$$

The Lagrange functional L for this problem is expressed as

$$L(A, \Omega) = \int_A dA + \Lambda_\Omega \left(\int_\Omega d\Omega - \hat{\Omega}\right). \tag{15}$$

The material derivative $\dot{L}$ of the Lagrange functional L with respect to shape variation is expressed as

$$\dot{L} = <\boldsymbol{G}_A n, \boldsymbol{V}>_A + \Lambda'_\Omega \left(\int_\Omega d\Omega - \hat{\Omega}\right), \quad \boldsymbol{V} \in C_\Theta, \tag{16}$$

$$G_A = H_A + \Lambda_\Omega. \tag{17}$$

When the constraint condition with regard to the internal volume is met, Eq. (16) can be written as

$$\dot{L} = <\boldsymbol{G}_A n, \boldsymbol{V}>_A, \quad \boldsymbol{V} \in C_\Theta. \tag{18}$$

Eq. (17) and (18) imply that when the Lagrange functional L has the minimum (i.e. $\dot{L} = 0$), the mean curvatures have a constant value $-\Lambda_\Omega$ throughout the surface.

5.3. Suspension membrane structure problem

Consider the problem for minimizing the area of a suspension membrane structure is shown in Fig. 1(c). Setting up respectively specified fixed points on the boundary as the geometric constraint condition and a perimeter Γ of the boundary as the equality constraint condition (the constraint value is represented as $\hat{\Gamma}$), this problem is expressed as

$$\text{Given} \quad A_0, \tag{19}$$
$$\text{find} \quad \boldsymbol{V} \ (\text{or } A_s), \tag{20}$$
$$\text{that minimizes} \quad A \left(=\int_A dA\right), \tag{21}$$
$$\text{subject to} \quad \Gamma \left(=\int_{\partial A} d\Gamma\right) = \hat{\Gamma}. \tag{22}$$

The Lagrange functional L for this problem is represented as

$$L(A, \Gamma) = \int_A dA + \Lambda_\Gamma \left(\int_{\partial A} d\Gamma - \hat{\Gamma}\right). \tag{23}$$

If the constrained perimeter condition is met, the material derivative $\dot{L}$ of the Lagrange functional L with respect to shape variation is represented as

$$\dot{L} = <\boldsymbol{G}_A n, \boldsymbol{V}>_A + <\boldsymbol{G}_{\partial A} t, \boldsymbol{V}>_{\partial A}, \quad \boldsymbol{V} \in C_\Theta, \tag{24}$$

$$G_A = H_A, \quad G_{\partial A} = 1 + \Lambda_\Gamma H_{\partial A}. \tag{25)(26}$$

The shape gradient functions derived here are used for determining the optimal shape (or the optimal design velocity field or the optimal shape variation). We will explain the method in the next chapter.

6. Free-form optimization method for form-finding of membrane

The free-form optimization method was developed by the authors, and solutions to the optimal shape design problem of shell [9] and frame structure [10] have been proposed so far. This distributed-parameter shape optimization method is based on the traction method [11] which is a gradient method in a Hilbert space, and can deal with all nodes as the design variables without parameterization. In this study, we apply the free-form optimization method for shells with respect to the in-plane variation [8] and the out-of-plane variation so as to find an optimal free-form of membrane, i.e. minimal surface.

In order to determine the design velocity field that minimize the objective functional using both the derived shape gradient function and the gradient method in a Hilbert space, a tensor with positive definitiveness must be introduced. Unfortunately, a unit matrix only having diagonal component cannot maintain the smoothness of the shape since it leads to jagged problem [12]. For this reason, a stiffness matrix of elastic shell under the Robin condition similar to membrane in the shape is used for this method, which makes the computation simple, i.e. linear computation. This stiffness tensor serves not only to maintain the mesh smoothness, but also to restrain the rigid motion. With the optimal design velocity field $\boldsymbol{V}$ obtained by applying the distributed external forces in proportion to the negative shape gradient function to this pseudo-elastic shell, the reference shape is updated. Consider the design velocity field $\boldsymbol{V} = \{V_i\}_{i=1,2,3}$ divided between in-plane component $\boldsymbol{V}_0 = \{V_{0_\beta}\}_{\beta=1,2}$ and out-of-plane component V_3 on the local coordinate systems. Using the Kirchhoff's theory as a plate bending theory, the each governing equation of the design velocity field is explained as Eq. (27) and (29), respectively. In the case of the in-plane variation, the out-of-plane velocity field needs to be constrained (i.e. $V_3 = 0$). Therefore after the each design field is determined separately, they are synthesized as required with the relation $\boldsymbol{V} = \boldsymbol{V}_n + \boldsymbol{V}_t$. Fig.3 shows the schematics of the velocity analysis for (a) out-of-plane shape variation and (b) in-plane shape variation.

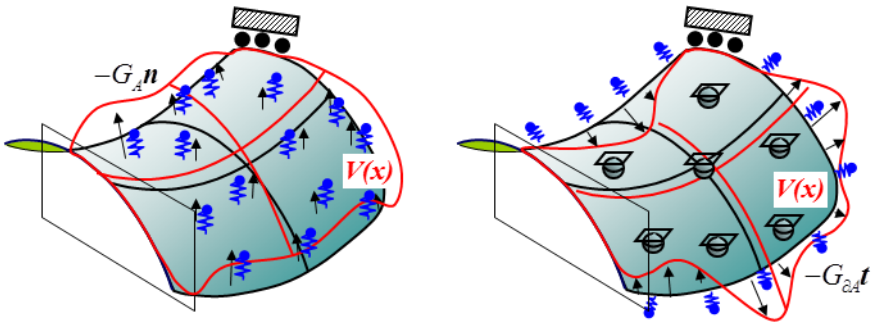

(a) Out-of-plane shape variation (b) In-plane shape variation

Figure 3: Schematics of the free-form optimization method for membrane

$$a((\boldsymbol{V}_{0\beta}, V_3, \boldsymbol{\theta}), (\bar{\boldsymbol{u}}_0, \bar{w}, \bar{\boldsymbol{\theta}})) + \alpha \left\langle (\boldsymbol{V}\cdot\boldsymbol{n})\boldsymbol{n}, (\bar{\boldsymbol{u}}_0, \bar{w}, \bar{\boldsymbol{\theta}}) \right\rangle_A = -< \boldsymbol{G}_A n, (\bar{\boldsymbol{u}}_0, \bar{w}, \bar{\boldsymbol{\theta}}) >_A,$$
$$(\boldsymbol{V}_{0\beta}, V_3, \boldsymbol{\theta}) \in C_\Theta, \quad \forall (\bar{\boldsymbol{u}}_0, \bar{w}, \bar{\boldsymbol{\theta}}) \in C_\Theta, \qquad (27)$$

$$C_\Theta = \{(V_{0_1}, V_{0_2}, V_3, \theta_1, \theta_2) \in (H^1(A))^5 \,|\, (\boldsymbol{V}_0, V_3, \boldsymbol{\theta}) \textit{ satisfy the constraints of shape variation on } A\}. \qquad (28)$$

$$a((\boldsymbol{V}_{0\beta}, V_3, \boldsymbol{\theta}), (\bar{\boldsymbol{u}}_0, \bar{w}, \bar{\boldsymbol{\theta}})) + \alpha \left\langle (\boldsymbol{V}\cdot\boldsymbol{t})\boldsymbol{t}, (\bar{\boldsymbol{u}}_0, \bar{w}, \bar{\boldsymbol{\theta}}) \right\rangle_{\partial A} = -< \boldsymbol{G}_{\partial A} t, (\bar{\boldsymbol{u}}_0, \bar{w}, \bar{\boldsymbol{\theta}}) >_{\partial A},$$
$$(\boldsymbol{V}_{0\beta}, V_3, \boldsymbol{\theta}) \in C_\Theta, \quad \forall (\bar{\boldsymbol{u}}_0, \bar{w}, \bar{\boldsymbol{\theta}}) \in C_\Theta, \qquad (29)$$

$$C_\Theta = \{(V_{0_1}, V_{0_2}, V_3, \theta_1, \theta_2) \in (H^1(A))^5 \,|\, (\boldsymbol{V}_0, V_3, \boldsymbol{\theta}) \textit{ satisfy the constraints of shape} \text{ variation on } S \textit{ and } V_3 = 0 \textit{ on } A\}. \qquad (30)$$

Here, the bilinear form $a(\cdot\,,\,\cdot)$ which represents virtual work related to internal force and the linear forms $<\cdot\,,\,\cdot>_A$, $<\cdot\,,\,\cdot>_{\partial A}$ are expressed as Eq. (31) and Eq.(32), (33), respectively. $\bar{(\,)}$ and C_Θ express the variation and the admissible function space which satisfies the constraints of shape variation for shape design, respectively.

$$a((\boldsymbol{u}_0, w, \boldsymbol{\theta}), (\bar{\boldsymbol{u}}_0, \bar{w}, \bar{\boldsymbol{\theta}})) = \int_A \{c^B_{\alpha\beta\gamma\delta}\kappa_{\gamma\delta}\bar{\kappa}_{\alpha\beta} + c^M_{\alpha\beta\gamma\delta}\varepsilon_{0\gamma,\delta}\bar{\varepsilon}_{0\alpha,\beta}\} dA, \qquad (31)$$

$$< \boldsymbol{G}_A n, (\bar{\boldsymbol{u}}_0, \bar{w}, \bar{\boldsymbol{\theta}}) >_A = \int_A G_A \bar{w} dA\,, \tag{32}$$

$$< \boldsymbol{G}_{\partial A} t, (\bar{\boldsymbol{u}}_0, \bar{w}, \bar{\boldsymbol{\theta}}) >_{\partial A} = \int_{\partial A} (G_{\partial A_\beta} \bar{u}_{0\beta}) d\Gamma\,, \tag{33}$$

where w and $\boldsymbol{u}_0 = \{u_{0\alpha}\}_{\alpha=1,2}$ represent the out-of plane displacement and the in-plane displacement vector at the center plane, respectively. $\{\kappa_{\alpha\beta}\}_{\alpha,\beta=1,2}$ and $\{\varepsilon_{0\alpha\beta}\}_{\alpha,\beta=1,2}$ represent the curvature tensor and the strain tensor at the center plane, respectively, which are defined as

$$\kappa_{\alpha\beta} \equiv \frac{1}{2}(w_{,\alpha\beta} + w_{,\beta\alpha}), \qquad \varepsilon_{0\alpha\beta} \equiv \frac{1}{2}(u_{0\alpha,\beta} + u_{0\beta,\alpha})\,. \tag{34)(35}$$

The fact that the shape variation due to the design velocity field $\boldsymbol{V}$ obtained in the velocity analysis, i.e. Eq. (27) and/or Eq. (29), decreases the objective functional, is verified as noted below. In the case of Eq. (27), when the constraint condition equation is met, the perturbation expansion of the Lagrange objective functional $\boldsymbol{L}$ is written as

$$\Delta L = \left\langle G_A \boldsymbol{n}, \Delta s(\boldsymbol{V}, \boldsymbol{\theta}) \right\rangle_A + O(|\Delta s|^2)\,. \tag{36}$$

Substituting Eq. (30) into Eq. (32) and taking account of the positive definitiveness of $a((\boldsymbol{V}_{0\alpha}, V_3, \boldsymbol{\theta}), (\bar{\boldsymbol{u}}_0, \bar{w}, \bar{\boldsymbol{\theta}}))$ and $\alpha\left\langle (\boldsymbol{V}\cdot\boldsymbol{n})\boldsymbol{n}, (\bar{\boldsymbol{u}}_0, \bar{w}, \bar{\boldsymbol{\theta}}) \right\rangle$, Eq.(37) can be obtained if Δs is sufficiently-small.

$$\Delta L = -\{a(\Delta s(\boldsymbol{V}, \boldsymbol{\theta}), \Delta s(\boldsymbol{V}, \boldsymbol{\theta})) + \alpha \left\langle (\Delta s \boldsymbol{V}\cdot\boldsymbol{n})\boldsymbol{n}, \Delta s(\boldsymbol{V}, \boldsymbol{\theta}) \right\rangle_A\} < 0\,. \tag{37}$$

The same approach can be applied to the case of Eq. (29). These relations indicate that, on the problem having the convexity, the Lagrange objective functional $\boldsymbol{L}$ is necessarily decreased by updating the shape according to the velocity field $\boldsymbol{V}$ determined in the velocity analysis. We use the method proposed as a solution to a multiconstraint problem by the traction method [13] in order to satisfy the constraint conditions (e.g. internal volume and perimeter) according to the type of the membrane structure.

The minimal surface with the optimal free-form can be obtained by repeating the three processes: (i) computation of the shape gradient function, (ii) velocity analysis and (iii) shape updating. In this study, the general-purpose FEM code is used in the velocity analysis.

7. Computed results of minimal surface

7.1. Frame membrane structure problem (Area minimization)

In order to verify the validity of this form-finding method for frame membrane structures, it was applied to a problem which finds a catenoid known as one of the minimal surfaces. The initial shape of a cylinder, both ends of which were framed as the specified boundaries is shown in Fig. 4(a). In the velocity analysis the boundaries were simply supported. By the out-of-plane variation according to the shape gradient function, i.e. Eq.(15), the minimal shape shown in Fig. 4(b) was determined. Fig. 5 and Fig. 6 show the iteration convergence histories of the area and the mean curvatures of the optimal shape along A-B. The results show that the shape obtained is a well-approximated catenoid with smoothness. The area decreased by around 7% and converged steadily while the mean curvatures were almost vanished similar to the theoretical value. From the results, validity of this form-finding method for frame membrane structures was verified.

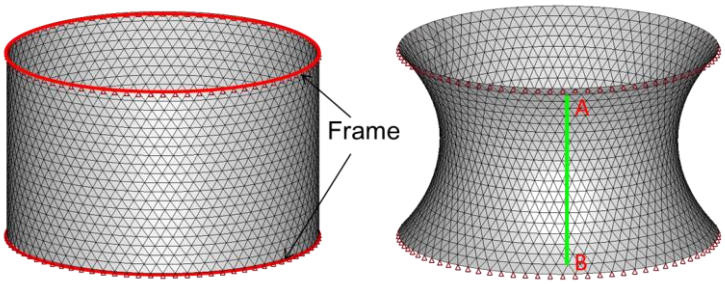

(a) Initial shape (b) Optimal shape

Figure 4: Optimization result of frame membrane structure (catenoid)

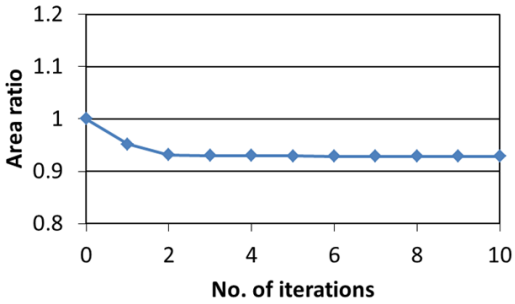

Figure 5: Iteration histories of frame membrane structure (catenoid)

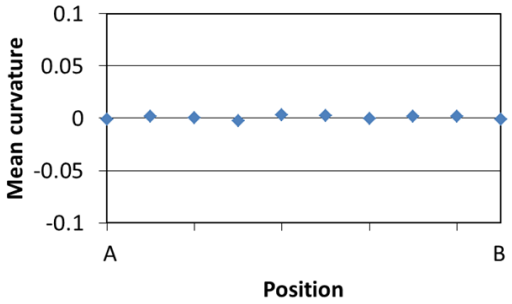

Figure 6: Mean curvatures along A-B of frame membrane structure (catenoid)

7.2. Pneumatic membrane structure problem with frame (Area minimization subjected to internal volume constraint)

The proposed method is applied to a pneumatic membrane structure combined with frame structure. The initial shape of hemisphere, the surface of which was partly framed and the bottom edge of which was fixed as a specified boundary is shown in Fig. 7(a). The internal volume constraint was set as 120% of the initial shape. In the velocity analysis, the boundary was simply supported. By the out-of-plane variation according to the shape gradient function, i.e. Eq.(23), the minimal surface was determined. The internal volume was computed by space discretization using tetra elements. Fig. 7(b) shows the optimal shape obtained. The smooth shape was created. Fig. 8 shows the iteration convergence histories of the area and the internal volume, while Fig. 9 shows the mean curvatures of the final shape along A-B.

The graphs show that the area was minimized yet increased by around 15% as the internal volume constraint was satisfied, while the mean curvatures have the constant value. From the results, it was verified that the valid result for pneumatic membrane structure subjected to an internal volume constraint can be obtained.

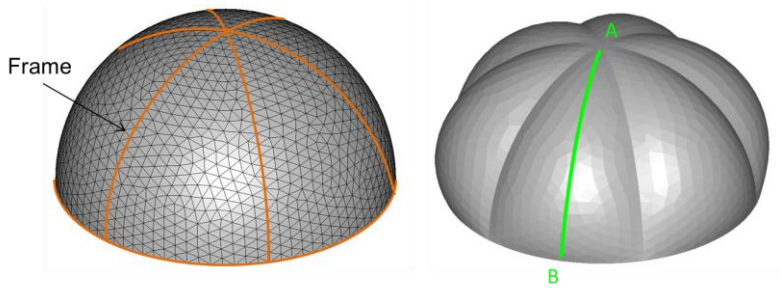

(a) Initial shape (b) Optimal shape

Figure 7: Optimization result of pneumatic membrane structure with frame

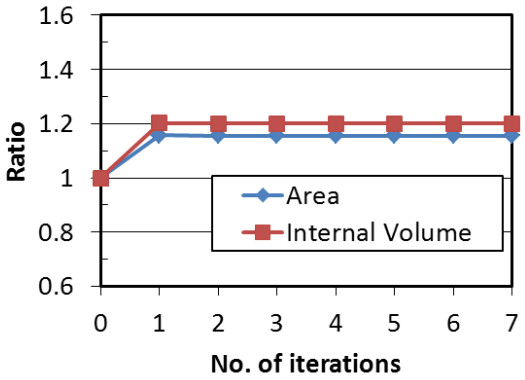

Figure 8: Iteration histories of pneumatic membrane structure with frame

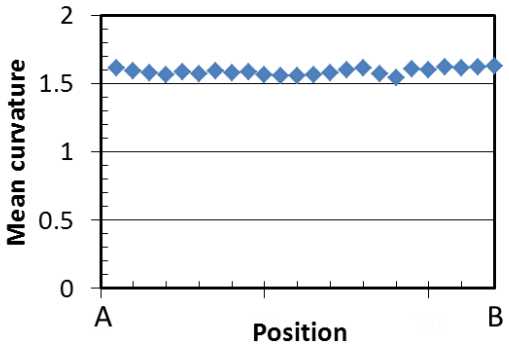

Figure 9: Mean curvatures along A-B of pneumatic membrane structure with frame

7.3. Suspension membrane structure problem (Area minimization subjected to perimeter constraint)

The initial shape, the five vertexes of which were fixed is shown in Fig. 10(a). Under a perimeter constraint condition, the area minimization analysis was conducted. In the velocity analysis, the fixed points were simply supported. By the out-of-plane and in-plane variations according to the shape gradient functions, i.e. Eq.(31) and Eq. (32), the minimal surface was determined. The perimeter constraint was set as 120% of the initial shape. Fig. 10(b) shows the optimal shape obtained. The area was minimized and decreased by around 58%, while the perimeter constraint was satisfied. The smooth surface and boundary shape having the almost constant curvatures was obtained.

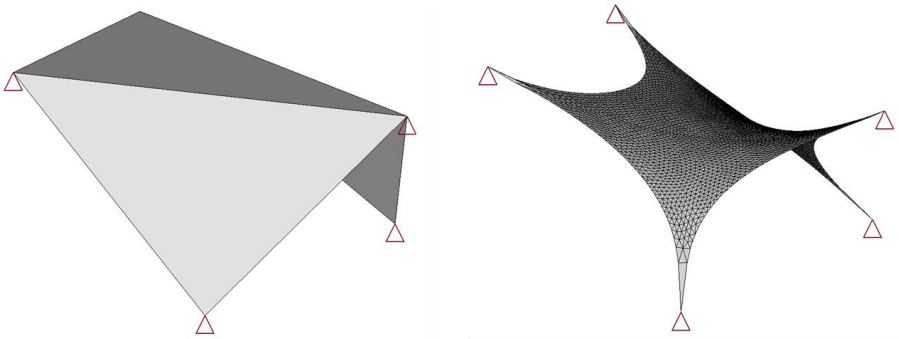

(a) Initial shape (b) Optimal shape

Figure 10: Optimization result of spatial suspension membrane structure

8. Conclusions

In this paper, we formulated various form-finding problems of membrane as the distributed-parameter shape optimization problems aiming at equally tensioned surface (i.e. minimal surface) which is essential for the membrane design, and proposed a new numerical solution for finding the optimal shape. This is what the previously-reported free-form optimization method for shells were applied to membrane structures. According to the type of membrane structure (e.g. frame membrane structure, pneumatic membrane structure and suspension structure), the in-plane shape variation and/or the out-of-plane shape variation was set as the variable for the form-finding. Applying the derived sensitivity function to the gradient method in a Hilbert space and determining the optimal design velocity field based on the assumption of small variation, we found the minimal surfaces by the iterative computation. With this method, the optimal and smooth free-forms of membranes can be obtained without shape parameterization. The validity and the versatility of the proposed method were verified by the result of the examples for the each type of membrane structure.

9. References

[1] F. Otto, *Tensile Structures*, MIT Press, 1973.

[2] A. Gray, *Modern Differential Geometry of Curves and Surfaces with MATHEMATICA*, CRC Press, 1998.

[3] J. Monterde, Bézier Surfaces of Minimal Area: The Dirichlet Approach, *Computer Aided Geometric Design*, 21(2), 117–136, 2004.

[4] A. Arnal, A. Lluch and J. Monterde, Triangular Bézier Approximations to Constant Mean Curvature surfaces, *Computational Science – ICCS 2008*, 5102, 96-105, 2008.

[5] K. U. Bletzinger, M. Firl, J. Linhard and R. Wuchner, Optimal Shapes of Mechanically Motivated Surfaces, *Computer Methods in Applied Mechanics and Engineering*, 199(5-8), 324-333, 2010.

[6] K. U. Bletzinger, R. Wuchner, F. Daoud, and N. Camprubi, Computational Methods for Form Finding and Optimization of Shells and Membranes, *Computer Methods in Applied Mechanics and Engineering*, 194(30-33), 3438-3452, 2005.

[7] M. Shimoda, H. Azegami and T. Sakurai, Traction Method Approach to Optimal Shape Design Problems, *SAE 1997 Transactions, Journal of Passenger Cars*, Section 6, 106, 2355-2365, 1998.

[8] M. Shimoda, and J Tsuji, Non-parametric Shape Optimization Method for Rigidity Design of Automotive Sheet Metal Structure, SAE Technical Paper, 2006.

[9] M. Shimoda, K. Ishikawa and H. Azegami, A Shape Optimization Method for the Optimal Free-form Design of Shell Structure, CD-proceedings of 8th World Congress on Structural and Multidisciplinary Optimization, 2009.

[10] M. Shimoda, Y. Liu and F. Hayashi, Free-form Optimization Method for Designing Spatial Frame Structure, 10th World Congress on Structural and Multidisciplinary Optimization, 2013.

[11] H. Azegami, A Solution to Domain Optimization Problems, *Trans. of Jpn. Soc. of Mech. Eng.*, 60, 1479-1486, 1994 (in Japanese).

[12] V. Braibant and C. Fleury, Shape Optimal Design Using B-splines, Computer Methods in Applied Mechanics and Engineering, 44(3), 247-267, 1984.

[13] M. Shimoda, H. Azegami and T. Sakurai, Shape Optimization of Linear Elastic Structures Subject to Multiple Loading Conditions, *Current Topics in Computational Mechanics*, 305, 319-326, 1995.